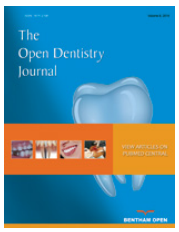

The Open Dentistry Journal

Content list available at: https://opendentistryjournal.com

RESEARCH ARTICLE

Assessment of Trabecular Bone During Dental Implant Planning using Cone-beam Computed Tomography with High-resolution Parameters

Lauren Bohner[1,2,*], Pedro Tortamano[1], Felix Gremse[3], Israel Chilvarquer[4], Johannes Kleinheinz[2] and Marcel Hanisch[2]

[1]*Department of Prosthodontics, School of Dentistry, University of São Paulo, Av. Lineu Prestes 2227, 05508-000, São Paulo, Brazil*
[2]*Department of Cranio-Maxillofacial Surgery, University Hospital Muenster, Albert-Schweitzer-Campus 1, 48149, Muenster, Germany*
[3]*Department of Experimental Molecular Imaging, Helmholtz Institute, RWTH Aachen University, Forckenbeckstraße 55, 52074, Aachen, Germany*
[4]*Department of Stomatology, School of Dentistry, University of São Paulo, Av. Lineu Prestes 2227, 05508-000, São Paulo, Brazil*

Abstract:

Background:

Cone-Beam Computed Tomography (CBCT) with high-resolution parameters may provide an acceptable resolution for bone assessment.

Objectives:

The purpose of this study is to assess trabecular bone using two cone-beam computed tomography (CBCT) devices with high-resolution parameters in comparison to micro-computed tomography (µCT).

Methods:

Bone samples (n=8) were acquired from dry mandibles and scanned by two CBCT devices: 1) VV (Veraview R100, Morita; FOV 4x4, 75kV, 9mA, voxel size 0.125µm); and PR (Prexion 3D, Prexion; FOV 5x5, 90kV, 4mA, 37s, voxel size 108µm). Gold-standard images were acquired using µCT (SkyScan 1272; Bruker; 80kV, 125mA, voxel size 16µm). Morphometric parameters (BvTv- Bone Volume Fraction, BsBv- Trabecular specific surface, TbTh- Trabecular thickness and TbSp- Trabecular separation) were measured. Statistical analysis was performed within ANOVA, Spearman Correlation test and Bland-Altmann plots with a statistical significance level at p=0.05.

Results:

CBCT devices showed similar BvTv values in comparison to µCT. No statistical difference was found for BvTv parameters assessed by CBCT devices and µCT. BsBv values were underestimated by CBCT devices ($p<0.01$), whereas TbTh and TbSp values were overestimated by them ($p<0.01$). Positive correlations were found between VV and µCT measurements for BvTv ($r^2= 0.65$, $p=0.00$), such as between PR and µCT measurements for TbSp ($r^2= 0.50$, $p=0.04$). For BsBv measurements, PR was negatively correlated with µCT ($r^2= -0.643$, $p=0.01$).

Conclusion:

The evaluated CBCT device was able to assess trabecular bone. However, bone parameters were under or overestimated in comparison to µCT.

Keywords: Cone-Beam computed tomography, Microcomputed tomography, MicroCT, X-ray microCT, Facial bone, Trabecular bone, Dental implants.

Article History	Received: September 24, 2020	Revised: December 28, 2020	Accepted: January 7, 2021

1. INTRODUCTION

One important factor for successful dental implant treatment is the choice of an optimal site for the planned prosthetic and surgical reconstruction [1 - 5]. In this respect, not only the position of the implant-supported restoration but also the bone features should be taken into consideration [6]. Recent studies have shown that trabecular bone micro-architecture may influence the primary stability of dental implants [7, 8]. Hence, assessment of trabecular bone has also been gaining special attention [3, 9, 10].

Clinically, Cone-beam Computed Tomography (CBCT) is

* Address correspondence to this author at Department of Cranio-Maxillofacial Surgery, University Hospital Muenster, Albert-Schweitzer-Campus 1, 48149, Muenster, Germany, Phone: +49 251 83-47004 Fax: +49 251 83-47184, E-mail: lauren.bohner@ukmuenster.de

the method of choice to evaluate bone [10 - 12]. Whereas cortical bone measurements can be precisely determined by CBCT [13]; limitations of the technique, as excessive noise and hardening beam artifacts, may hamper the assessment of trabecular bone [14, 15].

Despite the limitations related to the technique, a recent study reported an acceptable accuracy for the assessment of trabecular bone. Due to the range of available resolution parameters, these findings may not be extended to all CBCT devices. However, it is expected that high-resolution parameters may provide higher accuracy for bone assessment.

Due to the capability of the technique of providing images with a spatial resolution up to 2 μm, microcomputed tomography (μCT) is considered the gold-standard technique to evaluate jaw bone in laboratory research works . The technique allows determining both bone volume and trabecular morphology [16]. This study proposed to compare the trabecular bone assessment by two CBCT devices in regard to the μCT. The null hypothesis is that there is no difference in trabecular bone parameters acquired from μCT and CBCT devices.

2. MATERIALS AND METHODS

2.1. Study Design

The present study was performed after approval of the Ethics Committee of School of Dentistry, University of São Paulo (Protocol number 2.253.943). Trabecular bone was assessed using two CBCT scanners. Two types of bone were considered: Group 1 (G1) consisted of non-prepared bone, whereas group 2 (G2) consisted of decalcified bone, representing a bone loss situation.

Measurements were compared with gold standard measurements provided by micro-computed tomography (μCT). The following bone morphological parameters were assessed [17]:

- Trabecular volume fraction (BvTv): the ratio (%) of segmented trabecular bone volume (BV) to the total volume;
- Bone specific surface (BsBv): Ratio (1/cm) of segmented trabecular bone surface (BS) to the trabecular bone volume (BV);
- Trabecular thickness (TbTh): Mean thickness of trabecular bone (cm)
- Trabecular separation (TbSp): Mean distance between trabeculae (cm)

The sample size was determined based on BvTv and TbTh, since these were considered the main parameters for bone assessment. A pilot study (n=3) was performed and the number of required samples was calculated using G*Power app (Dusseldorf). According to the test, at least eight samples were required to identify a mean difference of 15±4.27% of BvTv and 0.02cm of TbTh with a significance of 0.05 and α= 80%.

2.2. Samples Acquisition

Four human dry mandibles were provided by the Department of Anatomy, Biomedical Sciences Institute of the University of São Paulo. These were sectioned in bone samples measuring 3 cm in length using a diamond disc. Four bone samples were extracted from each mandible, two from the anterior mandible and two from the posterior mandible.

Bone samples were divided into two groups (n=8) according to the bone type: G1 contained bone samples acquired from the anterior mandible, which consists of a more dense bone. G2 represented a bone loss situation; thus, bone samples were acquired from the posterior mandible and decalcified according to the protocol described by Hua et al. (2009) [18]. In summary, samples were immersed in hydrocloridric acid (HCl) solution (Decal, Serva, Heidelberg, Germany) twice, for ten minutes each time. After each interval, samples were rinsed with distilled water and dried.

The difference between bone parameters of groups G1 and G2 was first controlled by scanning the samples with a microcomputed tomography Skyscan 1272 (Bruker, Kontich, Belgium). The following parameters were used: 80kV, 125mA and voxel size 16μm [19]. Bone parameters were calculated and the difference between the groups was confirmed by Student`s t test (Appendix **1**). The same parameters were used as control (gold-standard).

2.3. Cone-beam Computed Tomography

CBCT images were acquired with two high-resolution CBCT scanners:

VV- Veraviewpocs R100 (Morita), with a field of view (FOV) 4x4, 75kV, 9mA, voxel size of 0.125 μm; and PR-Prexion 3D (Prexion), with a field of view (FOV) of 5x5, 90kV, 4mA, 37s, and a voxel size of 108 μm.

2.4. Image Processing

Images were processed using the software Imalytics Preclinical (Gremse-IT GmbH, Aachen, Germany) [20]. Bone structures were matched using common points as reference. Regions were defined using a combination of manual and automated segmentation. First, cortical bone, trabecular bone, and marrow spaces were segmented and classified into different categories according to different threshold values.

Due to the high contrast among tissues in μCT images, it was possible to segment bone using a mean threshold value determined by the software. For CBCT groups, as the contrast was lower, this mean threshold value was not representative. In other words, since the tissue borders might not be well-delimited in CBCT images, a fixed threshold value could exceed the trabecular dimensions. Thus, for those cases, the threshold value was individually calculated for each image based on the grey values of bone and air. The segmentation was then visually inspected. When required, it was refined based on morphological parameters using distance mapping.

2.5. Trabecular Bone Assessment

A Volume Of Interest (VOI) comprising only trabecular bone was manually determined. Bone parameters cited above (BvTv, BsBv, TbTh, TbSp) were automatically calculated by the software Imalytics (Fig. **1a-d**). In addition, Standard

Tesselation Language (STL) tridimensional (3D) models representing the selected VOI were created and exported to the software GOM Inspect. A representative visual analysis was performed using a color-coded map to compare the experimental groups with the gold-standard (Fig. **2a-d**).

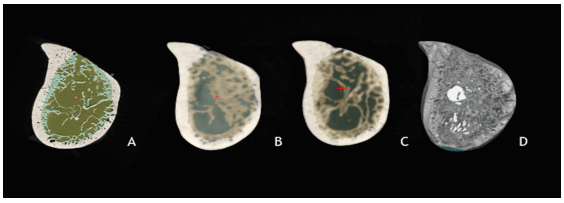

Fig. (1). Bone segmentation on cross-sectional images. (**a**). µCT. (**b**). Morita. (**c**). Prexion. (**d**). STL 3D-model from µCT.

2.6. Statistical Analysis

Descriptive data were described as mean ± standard deviation and 95% confidence interval (95% CI). Shapiro-Wilk was used to assess the adherence to the normal curve. In addition, the adherence to the Mauchly sphericity was assessed. Within-ANOVA and post-hoc tests were used to assess the statistical difference among scanners according to the bone type (G1 and G2).

The general accuracy of CBTs was evaluated by pooling groups G1 and G2 together. Bland-Altman plots were made to evaluate the general accuracy of CBCT scanners. The correlation of measurements obtained by each scanner to µCT was assessed using the non-parametric Spearman correlation test.

3. RESULTS

Table **1** describes data and statistical analysis of bone values assessed by CBCT according to each bone type. A significant interaction was shown between scanners and bone type for BvTv, BsBv and TbTh values (Appendix **1**).

Bone parameters assessed by CBCT and µCT are represented in Fig. (**3**). Measurements of BvTv and BsBv were underestimated by CBCT. However, for BvTv, this difference was not statistically significant (VV: p=0.13; PR: p=0.06). For BsBv, both scanners differed statistically from µCT (VV p= 0.00; PR p=0.01). Conversely, TbTh and TbSp were overestimated by both scanners (p<0.01).

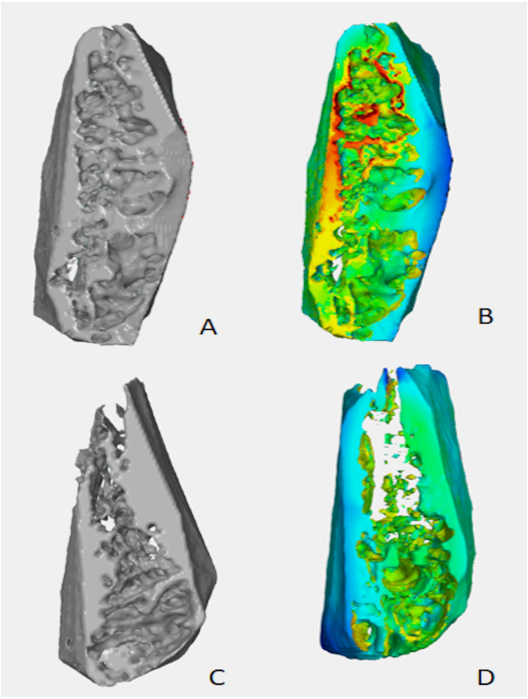

Fig. (2). STL 3D-models provided by CBCT in comparison with µCT-model. (**a**). A representative bone sample of G1. (**b**). A colour-coded deviation analysis between G1-sample and µCT-model. (**c**). A representative bone sample of G2. (**d**). A colour-coded deviation analysis between G2-sample and µCT-model.

Table 1. Descriptive data of µCT and CBCT measurements. SD = Standard deviation; 95% CI = 95% Confidence interval; BVTV = Trabecular volume fraction; BSBV = Bone specific surface; TbTh = Trabecular thickness; TbSp = Trabecular separation.

		uCT			VV			PR		
		Mean±SD	95%CI		Mean±SD	95%CI		Mean±SD	95%CI	
			Inferior	Superior		Inferior	Superior		Inferior	Superior
BV.TV										
	G1	53.17±12.57*	46.13	60.21	45.37±10.87*	38.91	51.84	37.86±9.13¶	32.45	43.27
	G2	33.51±3.78	26.47	40.54	32.57±5.20	26.10	39.03	36.55±4.29	31.14	41.96
BS.BV										
	G1	52.98±12.42*	43.19	62.78	20.05±3.77¶	16.32	23.78	34.65±5.78†	30.02	39.28
	G2	72.03±11.61*	62.87	81.19	27.25±5.15¶	23.76	30.74	27.44±5.56¶	23.11	31.77
TbTh										
	G1	0.06±0.01*	0.05	0.07	0.24±0.03¶	0.22	0.26	0.15±0.01†	0.13	0.17
	G2	0.05±0.01*	0.04	0.06	0.19±0.01¶	0.17	0.21	0.18±0.02¶	0.17	0.20
TbSp										
	G1	0.08±0.02*	0.06	0.10	0.27±0.08¶	0.21	0.33	0.19±0.06¶	0.14	0.24
	G2	0.12±0.02*	0.11	0.14	0.29±0.06¶	0.24	0.35	0.28±0.07¶	0.23	0.33

*¶† indicate statistical significant difference among scanners at p≤0.05.

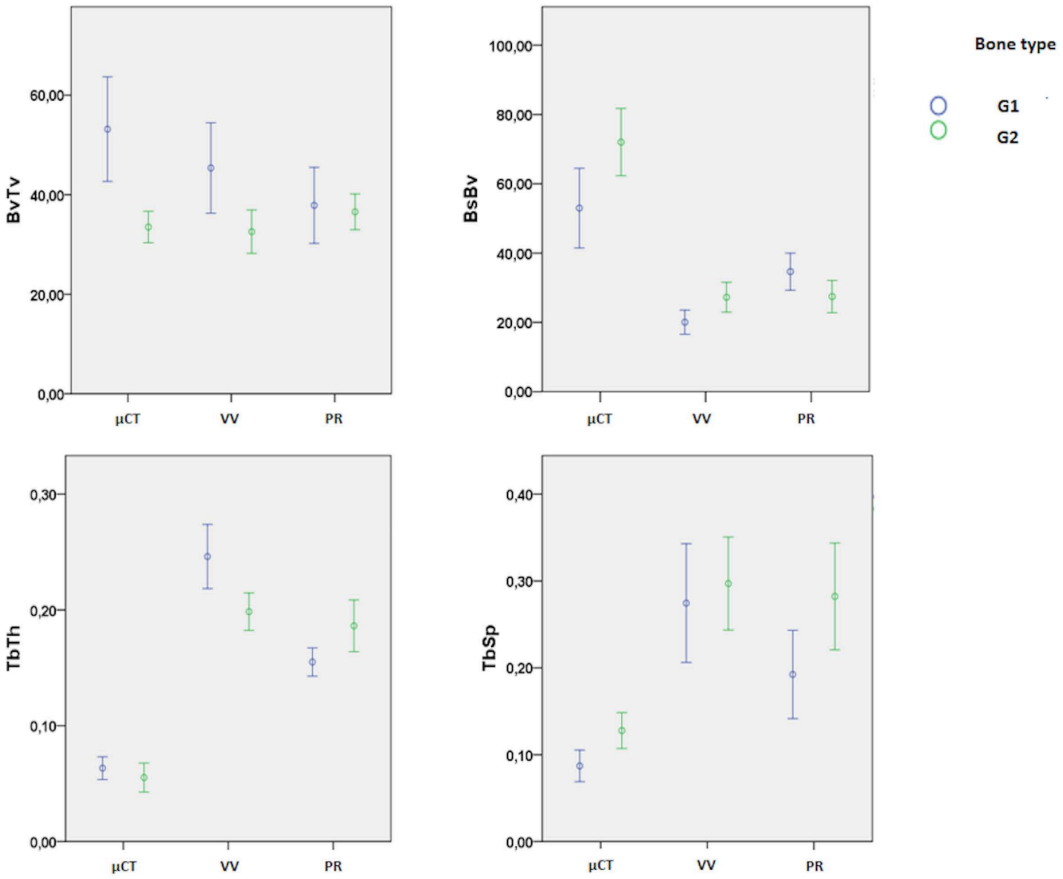

Fig. (3). Box-plots showing the measurements of trabeculae volume morphometry at anterior and posterior sites obtained by µCT (Gold-Standard) and CBCT scans. BVTV = Trabecular volume fraction; BSBV = Bone specific surface; TbTh = Trabecular thickness; TbSp = Trabecular separation.

Bland-Altman plots show the relationship between the arithmetic mean of CBCT and µCT measurements with the measurement error (µCT - CBCT measurements). Overestimated values by CBCT are shown as negative values (Fig. **4a-h**). The results suggested that for BsBv, the higher the mean values, the higher the underestimation by CBCT. Conversely, for TbSp, higher means are related to higher overestimated measurements.

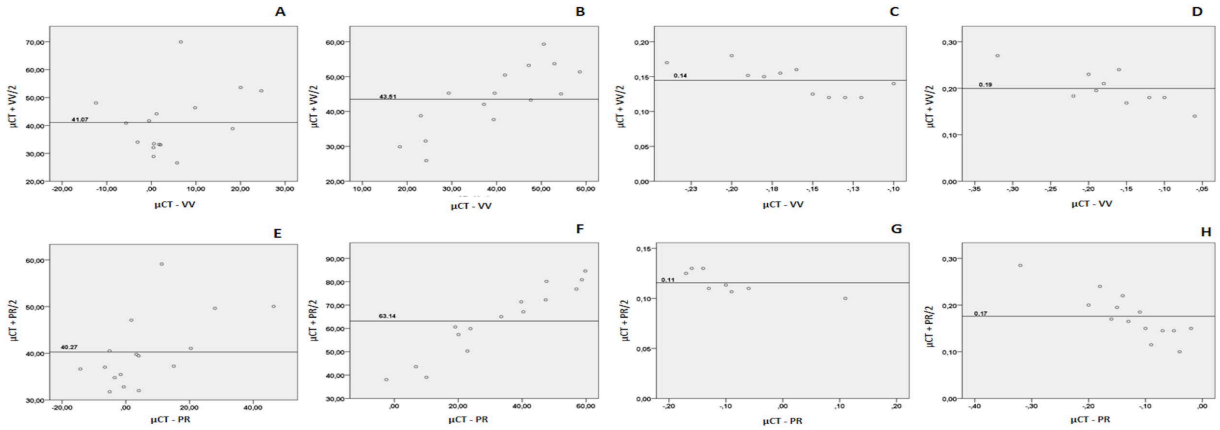

Fig. (4). Bland-Altman plots. (**a-d**). Measurements obtained by Morita; (**e-h**). Measurements obtained by Prexion. (**a**, **e**). Trabecular volume fraction (BVTV). (**b**,**f**). Bone specific surface (BSBV). (**c**,**g**) Trabecular thickness (TbTh). (**d**,**h**). Trabecular separation (TbSp).

There was a weak to moderate correlation between CBCT devices and μCT. A positive statistically significant correlation was found between VV and μCT (r_s=0.65, p=0.00) for BvTv, such as between PR and μCT measurements (r_s= 0.50, p=0.04) for TbSp values. For BsBv measurements, PR was negatively correlated with μCT (r_s= -0.643, p=0.01).

4. DISCUSSION

The present study aimed to determine whether bone architecture values provided CBCT could be comparable with the gold-standard μCT. The clinical relevance relies on providing data regarding the accuracy of CBCT to determine bone microarchitecture, which could improve dental implant planning. However, null hypotheses were rejected since bone values were under or overestimated by CBCT.

The trabecular bone assessment has gained special attention during implant planning. Studies reported that not only a high bone density but also the vascularization of bone marrow are important factors when considering the osteointegration of dental implants [8]. In this study, the main morphometric parameters were assessed to determine trabecular bone: trabecular volume fraction, bone-specific surface, trabecular thickness, and trabecular separation [16].

Jaw bone with well-structured trabeculae tends to present high bone volume fraction and trabecular thickness, associated with a low bone surface density and trabecular separation. According to Van Dessel *et al*., (2016) [15], this is the ideal condition for osteointegration of dental implants. In order to simulate different clinical situations, two types of bone were considered in this study. The first one represented a more dense intact bone, whereas the second one simulated a bone loss, on which trabeculae tended to be thinner.

According to the findings of this study, CBCT tended to underestimate BvTv and BsBv parameters, but overestimating TbTh and TbSp values. These results are in agreement with previous studies, which show measurement errors for different CBCT devices [2, 3, 21, 22].

From all measurements performed by CBCT scanners, bone volume fraction was the most reliable one, regardless of the evaluated bone type. The underestimation of BsBv was related to the limitations of CBCT in determining the complexity of trabeculae. Conversely, the trabecular thickness was overestimated by CBCT scans. This may be explained by the partial volume effect produced by CBCT scans. As the voxel size is greater than the spatial resolution, boundaries may not show an optimal delimitation. That leads to a distortion of boundaries and, subsequently, measurement errors from trabecular thickness [14, 20].

Likewise, the partial volume effect can explain why trabecular separation was overestimated. Since trabeculae smaller than the voxel size does not appear on the final image, this was set as marrow space, increasing the values of trabecular spaces [14, 20]. Additionally, a limitation of this technique that may have affected the final image is the manual selection of threshold parameters, which only enabled visual inspection [23].

The image resolution is determined by voxel size, which can vary between 90um to 400um [14]. For situations where a reduced Field of View (FOV) is sufficient, clinicians can benefit from a balance between high-resolution mode and reduced radiation [24, 25]. Nonetheless, even high-resolution CBCT is limited to measure trabecular bone parameters [26].

CONCLUSION

In order to facilitate the visualization of bone structure, 3D-models were rendered and compared based on visual analysis. 3D rendering is a simple way to visualize trabecular bone architecture and determine the ideal implant site. The use of STL 3D-models in combination with morphometric analysis was previously recommended to assist clinicians in choosing the ideal implant placement site [3, 15].

The main limitation of this study is the inability to represent a clinical situation. Since dry mandibles were used, the influence of soft tissue was not considered. Furthermore, the segmentation method based on a threshold value is still limited due to the low contrast of anatomical structures in CBCT images. The methodology used for bone assessment requires a precise determination of VOI and may not be reliable for the clinical practice.

AUTHOR´S CONTRIBUTIONS

L.B. and P.T. made contributions to the study conception; L.B., F.G., and IC. acquired and analysed data; J.K., L.B., and M.H. interpreted data and drafted the work. All authors approved the submitted version.

ETHICS APPROVAL AND CONSENT TO PARTICIPATE

The present study was approved by the Ethics Committee of School of Dentistry, University of São Paulo, Brazil (Protocol number 2.253.943).

HUMAN AND ANIMAL RIGHTS

All procedures followed were in accordance with the ethical standards of the responsible committee on human experimentation (institutional and national) and with the Helsinki Declaration of 1975, as revised in 2008.

CONSENT FOR PUBLICATION

Not applicable

AVAILABILITY OF DATA AND MATERIALS

The datasets used during the current study can be made available upon reasonable request to the corresponding author [L.B].

FUNDING

None.

CONFLICT OF INTEREST

The author declares no conflict of interest, financial or otherwise.

ACKNOWLEDGEMENTS

Not applicable.

APPENDIX

Appendix 1. Within-ANOVA results for all the evaluated parameters. df = degrees of freedom; BVTV = Trabecular volume fraction; BSBV = Bone specific surface; TbTh = Trabecular thickness; TbSp = Trabecular separation.

	Sum of Squares	df	Mean square	F	p-value
BvTv					
Scanner	319.027	2	159.51	2.23	0.12
Scanner*Bone	688.21	2	344.10	4.81	0.01
BsBv					
Scanner	12713.63	1.31	9693.20	93.14	0.00
Scanner* Bone	1290.74	1.31	984.09	9.45	0.00
TbTh					
Scanner	0.222	2	0.111	234.17	0.00
Scanner* Bone	0.012	2	0.006	13.11	0.00
TbSp					
Scanner	0.272	2	0.136	41.61	0.00
Scanner* Bone	0.010	2	0.005	1.48	0.24

REFERENCES

[1] Tey VHS, Phillips R, Tan K. Five-year retrospective study on success, survival and incidence of complications of single crowns supported by dental implants. Clin Oral Implants Res 2017; 28(5): 620-5. [http://dx.doi.org/10.1111/clr.12843] [PMID: 27334865]

[2] González-García R, Monje F. The reliability of cone-beam computed tomography to assess bone density at dental implant recipient sites: A histomorphometric analysis by micro-CT. Clin Oral Implants Res 2013; 24(8): 871-9. [http://dx.doi.org/10.1111/j.1600-0501.2011.02390.x] [PMID: 22250839]

[3] Van Dessel J, Nicolielo LF, Huang Y, *et al.* Accuracy and reliability of different cone beam computed tomography (CBCT) devices for structural analysis of alveolar bone in comparison with multislice CT and micro-CT. Eur J Oral Implantology 2017; 10(1): 95-105. [PMID: 28327698]

[4] Wakimoto M, Matsumura T, Ueno T, Mizukawa N, Yanagi Y, Iida S. Bone quality and quantity of the anterior maxillary trabecular bone in dental implant sites. Clin Oral Implants Res 2012; 23(11): 1314-9. [http://dx.doi.org/10.1111/j.1600-0501.2011.02347.x] [PMID: 22151688]

[5] Chrcanovic BR, Albrektsson T, Wennerberg A. Bone quality and quantity and dental implant failure: A systematic review and meta-analysis. Int J Prosthodont 2017; 30(3): 219-37. [http://dx.doi.org/10.11607/ijp.5142] [PMID: 28319206]

[6] Nicolielo LFP, Van Dessel J, van Lenthe GH, Lambrichts I, Jacobs R. Computer-based automatic classification of trabecular bone pattern can assist radiographic bone quality assessment at dental implant site. Br J Radiol 2018; 91(1092)20180437 [http://dx.doi.org/10.1259/bjr.20180437] [PMID: 30175923]

[7] Oh JS, Kim SG. Clinical study of the relationship between implant stability measurements using Periotest and Osstell mentor and bone quality assessment. Oral Surg Oral Med Oral Pathol Oral Radiol 2012; 113(3): e35-40. [http://dx.doi.org/10.1016/j.tripleo.2011.07.003] [PMID: 22669155]

[8] Ribeiro-Rotta RF, de Oliveira RC, Dias DR, Lindh C, Leles CR. Bone tissue microarchitectural characteristics at dental implant sites part 2: Correlation with bone classification and primary stability. Clin Oral Implants Res 2014; 25(2): e47-53. [http://dx.doi.org/10.1111/clr.12046] [PMID: 23106552]

[9] de Oliveira RC, Leles CR, Lindh C, Ribeiro-Rotta RF. Bone tissue microarchitectural characteristics at dental implant sites. Part 1: Identification of clinical-related parameters. Clin Oral Implants Res 2012; 23(8): 981-6. [http://dx.doi.org/10.1111/j.1600-0501.2011.02243.x] [PMID: 21722196]

[10] Jeong KI, Kim SG, Oh JS, Jeong MA. Consideration of various bone quality evaluation methods. Implant Dent 2013; 22(1): 55-9. [http://dx.doi.org/10.1097/ID.0b013e31827778d9] [PMID: 23287977]

[11] Sukovic P. Cone beam computed tomography in craniofacial imaging. Orthod Craniofac Res 2003; 6(Suppl. 1): 31-6. [http://dx.doi.org/10.1034/j.1600-0544.2003.259.x] [PMID: 14606532]

[12] Benic GI, Elmasry M, Hämmerle CH. Novel digital imaging techniques to assess the outcome in oral rehabilitation with dental implants: A narrative review. Clin Oral Implants Res 2015; 26(Suppl. 11): 86-96. [http://dx.doi.org/10.1111/clr.12616] [PMID: 26010421]

[13] Bohner LOL, Tortamano P, Marotti J. Accuracy of linear measurements around dental implants by means of cone beam computed tomography with different exposure parameters. Dentomaxillofac Radiol 2017; 46(5)20160377 [http://dx.doi.org/10.1259/dmfr.20160377] [PMID: 28267928]

[14] Scarfe WC, Farman AG. What is cone-beam CT and how does it work? Dent Clin North Am 2008; 52(4): 707-30. [http://dx.doi.org/10.1016/j.cden.2008.05.005] [PMID: 18805225]

[15] Van Dessel J, Nicolielo LF, Huang Y, *et al.* Quantification of bone quality using different cone beam computed tomography devices: Accuracy assessment for edentulous human mandibles. Eur J Oral Implantology 2016; 9(4): 411-24. [PMID: 27990508]

[16] Bouxsein ML, Boyd SK, Christiansen BA, Guldberg RE, Jepsen KJ, Müller R. Guidelines for assessment of bone microstructure in rodents using micro-computed tomography. J Bone Miner Res 2010; 25(7): 1468-86. [http://dx.doi.org/10.1002/jbmr.141] [PMID: 20533309]

[17] Dempster DW, Compston JE, Drezner MK, *et al.* Standardized nomenclature, symbols, and units for bone histomorphometry: A 2012 update of the report of the ASBMR Histomorphometry Nomenclature Committee. J Bone Miner Res 2013; 28(1): 2-17. [http://dx.doi.org/10.1002/jbmr.1805] [PMID: 23197339]

[18] Hua Y, Nackaerts O, Duyck J, Maes F, Jacobs R. Bone quality assessment based on cone beam computed tomography imaging. Clin Oral Implants Res 2009; 20(8): 767-71. [http://dx.doi.org/10.1111/j.1600-0501.2008.01677.x] [PMID: 19489931]

[19] Duttenhoefer F, Mertens ME, Vizkelety J, Gremse F, Stadelmann VA, Sauerbier S. Magnetic resonance imaging in zirconia-based dental implantology. Clin Oral Implants Res 2015; 26(10): 1195-202. [http://dx.doi.org/10.1111/clr.12430] [PMID: 24893967]

[20] Gremse F, Stärk M, Ehling J, Menzel JR, Lammers T, Kiessling F. Imalytics preclinical: Interactive analysis of biomedical volume data. Theranostics 2016; 6(3): 328-41. [http://dx.doi.org/10.7150/thno.13624] [PMID: 26909109]

[21] Pauwels R, Nackaerts O, Bellaiche N, *et al.* Variability of dental cone beam CT grey values for density estimations. Br J Radiol 2013; 86(1021)20120135

[http://dx.doi.org/10.1259/bjr.20120135] [PMID: 23255537]

[22] Van Dessel J, Huang Y, Depypere M, Rubira-Bullen I, Maes F, Jacobs R. A comparative evaluation of cone beam CT and micro-CT on trabecular bone structures in the human mandible. Dentomaxillofac Radiol 2013; 42(8)20130145
[http://dx.doi.org/10.1259/dmfr.20130145] [PMID: 23833320]

[23] Nackaerts O, Depypere M, Zhang G, Vandenberghe B, Maes F, Jacobs R. Segmentation of trabecular jaw bone on cone beam ct datasets. Clin Implant Dent Relat Res 2015; 17(6): 1082-91.
[http://dx.doi.org/10.1111/cid.12217] [PMID: 24629139]

[24] Bornstein MM, Scarfe WC, Vaughn VM, Jacobs R. Cone beam computed tomography in implant dentistry: A systematic review focusing on guidelines, indications, and radiation dose risks. Int J Oral Maxillofac Implants 2014; 29(Suppl.): 55-77.
[http://dx.doi.org/10.11607/jomi.2014suppl.g1.4] [PMID: 24660190]

[25] Bornstein MM, Horner K, Jacobs R. Use of cone beam computed tomography in implant dentistry: Current concepts, indications and limitations for clinical practice and research. Periodontol 2000 2017; 73(1): 51-72.
[http://dx.doi.org/10.1111/prd.12161] [PMID: 28000270]

[26] He RT, Tu MG, Huang HL, Tsai MT, Wu J, Hsu JT. Improving the prediction of the trabecular bone microarchitectural parameters using dental cone-beam computed tomography. BMC Med Imaging 2019; 19(1): 10.
[http://dx.doi.org/10.1186/s12880-019-0313-9] [PMID: 30674282]